Pharmaceutical Research, Vol. 23, No. 10, October 2006 (© 2006)
DOI: 10.1007/s11095-006-9023-4

Research Paper

Surface Crystallization of Indomethacin Below T_g

Tian Wu[1] and Lian Yu[1,2]

Received January 14, 2006; accepted March 29, 2006; published online August 23, 2006

Purpose. To study the surface crystallization of indomethacin (IMC) below T_g and its effects on the kinetics of overall crystallization.
Methods. Crystal growth rates in liquid layers formed between microscope cover glasses were measured with the top cover glass in place and removed. Polymorphs were identified by powder X-ray diffraction, Raman microscopy, and melting-point determination by hot-stage microscopy. Surface crystals were identified by scratching the sample surface, by cutting the sample to expose its interior, and by analyzing the intensity of X-ray diffraction. Amorphous IMC particles of different sizes were stored at 40°C (T_g−2°C) and analyzed at different times by differential scanning calorimetry to obtain the kinetics of crystallization.
Results. Crystal growth of IMC below T_g at the free surface was approximately two orders of magnitude faster than that in the bulk, resulting in a surface layer of crystals around a slower-crystallizing interior. Surface crystallization yielded mainly the γ polymorph. Amorphous IMC powders showed rapid initial crystallization at 40°C, but the crystallization abruptly slowed down at "saturation levels" below 100%; the larger the particles, the lower the "saturation level."
Conclusion. The faster surface crystallization of IMC than the bulk crystallization leads to unusual crystallization kinetics wherein a rapid initial increase of crystallinity is followed by an abrupt slowdown of crystallization. Surface crystallization should be distinguished from bulk crystallization in modeling and controlling the crystallization of amorphous solids.

KEY WORDS: amorphous solid; crystallization kinetics; glass transition; indomethacin; physical stability; surface crystallization.

INTRODUCTION

Surface crystallization has frequently been observed in studies of ceramic and metallic glasses (1,2) as distinct from bulk or internal crystallization. Such distinction, however, is rarely made in studies of amorphous pharmaceutical solids and their crystallization (3). Herein we report that the surface crystallization of indomethacin (a non-steroid anti-inflammatory, antipyretic and analgesic agent (4,5)) is faster than its bulk crystallization by orders of magnitude and this difference has significant effect on the overall kinetics of crystallization.

Indomethacin (IMC) is a model system for studying the stability and stabilization of pharmaceutical solids (6–10). IMC is known to crystallize below its glass transition temperature T_g (42°C), but the reported rates of crystallization vary widely. For example, at the room temperature (ca. T_g−20°C), the times of complete crystallization ranged from hours to years, depending in large part on how the sample was prepared: grinding of crystals (11–13), cooling of melt followed by grinding (6–8,12,13), and cooling of melt without grinding (7,14). At 40°C (T_g−2°C), the crystallization of IMC is apparently suspended after a fast start (8). These results show the inadequacy of the current understanding of crystallization near T_g and frustrate the efforts to predict and control the stability of amorphous solids.

Yoshioka *et al*., suggest that surface crystallization might explain certain unusual characteristics of IMC crystallization: "it appears that amorphous indomethacin under different conditions is responsive to some type of surface nucleation and growth" (8). Herein we provide the direct observation of the surface crystallization of IMC, which was significantly faster than the bulk crystallization and explains the fast initial rise of crystallinity followed by abrupt slowdown of crystallization.

MATERIALS AND METHODS

X-ray powder diffraction (XRPD) was performed with a Bruker D8 Advance X-ray diffractometer, which was equipped with a CuKα source (λ = 1.54056 Å) operating at a tube load of 40 kV and 40 mA. The divergence slit size was 1 mm, the receiving slit, 1 mm, and the detector slit, 0.1 mm. Data was collected by a high-resolution Sol-X detector. Each sample was scanned between 2 and 40° (2θ) with a step size of 0.02° and a maximum scan rate of 3 s/step. The NIST standard SRM 1976 was used to check the instrument's calibration and performance. Samples of small quantity were analyzed on a Si 510 zero-background holder. Polarized Light Microscopy (PLM) was performed with a Nikon Optiphot

[1] University of Wisconsin-Madison, School of Pharmacy, 777 Highland Ave., Madison, Wisconsin 53705-2222, USA.
[2] To whom correspondence should be addressed. (e-mail: lyu@pharmacy.wisc.edu)

Pol 2 microscope equipped with an Olympus video camera. The video image was calibrated against a 1 mm stage micrometer (100 divisions). Hot-stage measurements were performed with a Linkam THMS 600. Raman microscopy was performed with a Renishaw System 1000 Micro-Raman spectrometer equipped with a HeNe laser and peltier-cooled CCD detector. Differential scanning calorimetry (DSC) was conducted in crimped Al pans using a TA Instruments Q1000 unit under 50 mL/min N_2 purge.

Indomethacin [1-(*p*-chlorobenzoyl)-5-methoxy-2-methylindole-3-acetic acid, 99+%, IMC] was obtained from Sigma (St. Louis, MO) and used as received. The IMC received was the γ polymorph. A sample for studying surface crystallization was prepared by melting 3–5 mg of γ IMC at 175°C for 5 min on a clean microscope cover glass. The liquid was covered with another cover glass to yield a liquid layer ca. 15 μm thick and cooled to room temperature on an Al block. The resulting sample contained no crystals by PLM observation. To study crystallization at a free surface of the liquid, the top cover glass was removed at 22°C (T_g−20°C). To allow the free surface to relax and lose any strains from the previous contact with the top cover glass, the sample was annealed at 60°C (T_g+18°C) for 1 h. No crystals formed during this annealing. This annealing proved to have no significant effect on the rate of crystallization and was therefore omitted for the majority of the samples studied. For crystallization studies, the sample was stored in a clean dessicator loaded with Drierite® at a desired temperature (22–50°C, ± 1°C fluctuation). The extent of crystal growth was measured periodically at the room temperature, at which no significant growth occurred during the time of observation (the crystals grew at ca. 0.4 μm/hr at 22°C). For a crystal spherulite, the growth measurement was performed along four radii in orthogonal directions and the results were averaged. Two or three samples were measured at each temperature and for each sample, three spherulites were tracked over time. Depending on the size of the crystals, measurements were made at 40–400× magnifications. IMC polymorphs were identified by XRPD and melting-point measurement with the aid of a microscope hot stage. The chemical stability of IMC to melting was confirmed by the identical melting point of the recrystallized material. In this study, amorphous IMC showed T_g at 42°C while heated at 10°C/min, which agrees with previous reports (8).

To study the effect of particle size on overall crystallization rate, melt-quenched IMC was lightly ground in a mortar and sieved through 3" stainless steel sieves (Fisher scientific, USA) to yield three cuts: <75 μm (Sample S), 75–250 μm (Sample M), and >250 μm (Sample L). The samples were then stored at 40°C in a desiccator loaded with Drierite®. To determine their kinetics of crystallization, samples were periodically analyzed by DSC. Three milligrams of sample was withdrawn from Sample S, M, or L, placed in an Al pan, and scanned from −20 to 180°C. The heating rate of 10°C/min was used for Samples S and M and 3 or 5°C/min for Sample L (the heating rate was adjusted to ensure complete crystallization of the sample before melting). The fraction of uncrystallized IMC R was calculated from the heat of crystallization as follows:

$$R = \Delta H(t)/\Delta H_0 \tag{1}$$

where $\Delta H(t)$ is the heat of crystallization of the sample after storage time t and ΔH_0 is the heat of crystallization of a fully amorphous sample at the same crystallization temperature T_c. The value of ΔH_0 at a specific T_c was estimated from:

$$\Delta H_0 = \Delta H_m - \Delta C_p(T_m - T_c) \tag{2}$$

where ΔH_m is the enthalpy of fusion, T_m the melting temperature, and ΔC_p the heat capacity difference between liquid and crystal (assumed to be independent of T). We determined ΔC_p from a heating/cooling/reheating DSC run of a crystalline sample, which yielded a set of values of ΔH_m, ΔH_0, T_m, and T_c. The ΔC_p used in Eq. 2 was the average of three such determinations.

RESULTS AND DISCUSSION

An IMC liquid sandwiched between two cover glasses crystallized slowly below T_g. No crystallization was observed in unseeded samples in 6 months. With samples that had partially crystallized above T_g (e.g., during holding at 60°C) and been cooled to 40°C, it took 2 months for new, fiber-like crystals to become visible; the new crystals grew from or near the seeds at ca. 15 μm/month. In contrast, the same liquid with the top cover glass removed produced crystals in just 12 h at 40°C (Fig. 1a), in 1 day at 30°C, and in 5 days at 22°C. The number of crystals increased with the surface area, but not with the sample mass (thickness). These crystals were birefringent and transparent spherulites (Fig. 1a) of the γ polymorph. The polymorph was identified by Raman microscopy and melting-point measurement. Occasionally, the α polymorph was also observed as opaque spheruilites of fine fibers (Fig. 1b). The observed melting points of the γ and α

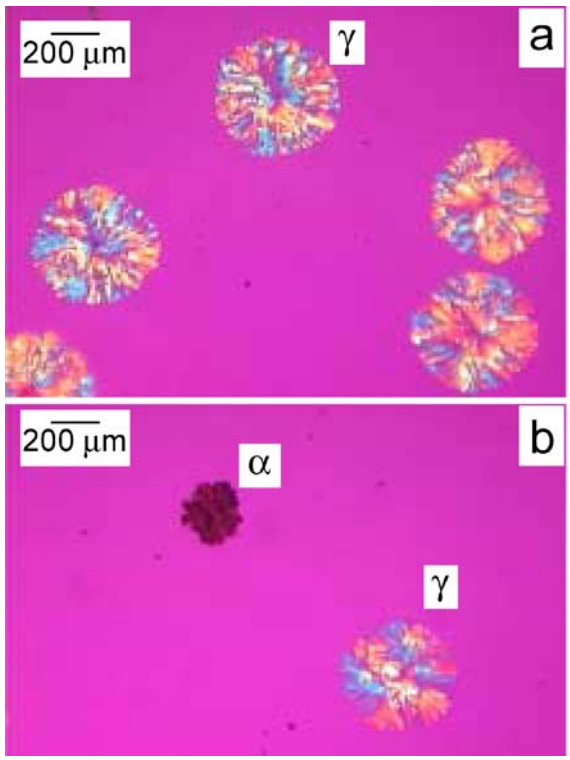

Fig. 1. Crystals appearing on the surface of amorphous IMC at 40°C. α and γ indicate IMC polymorphs.

polymorphs were 160 and 156°C, respectively, in agreement with previously published values (8). Figure 1a shows the typical density of nuclei at full coverage at 40°C. At lower temperatures, the density of nuclei was higher at full coverage because of the slower growth rates and the longer times available for nucleation to occur. Annealing at 60°C after the removal of the top cover glass, which was intended to release any strains from the previous contact with the cover glass, had no significant effect on the rate of nucleation or growth.

At 40°C, the entire surface of an 18×18 mm IMC sample was covered by crystals in approximately 3 weeks (Fig. 2a). This sample was then analyzed by XRPD. Surprisingly, the sample diffracted much more weakly (Fig. 2c) than a fully crystalline sample of comparable mass. After being heated at 140°C for 10 min, however, the sample diffracted more strongly (Fig. 2d), showing diffraction peaks characteristic of γ IMC. Compared to the sample before heating (Fig. 2a), the sample after heating appeared more opaque and to have

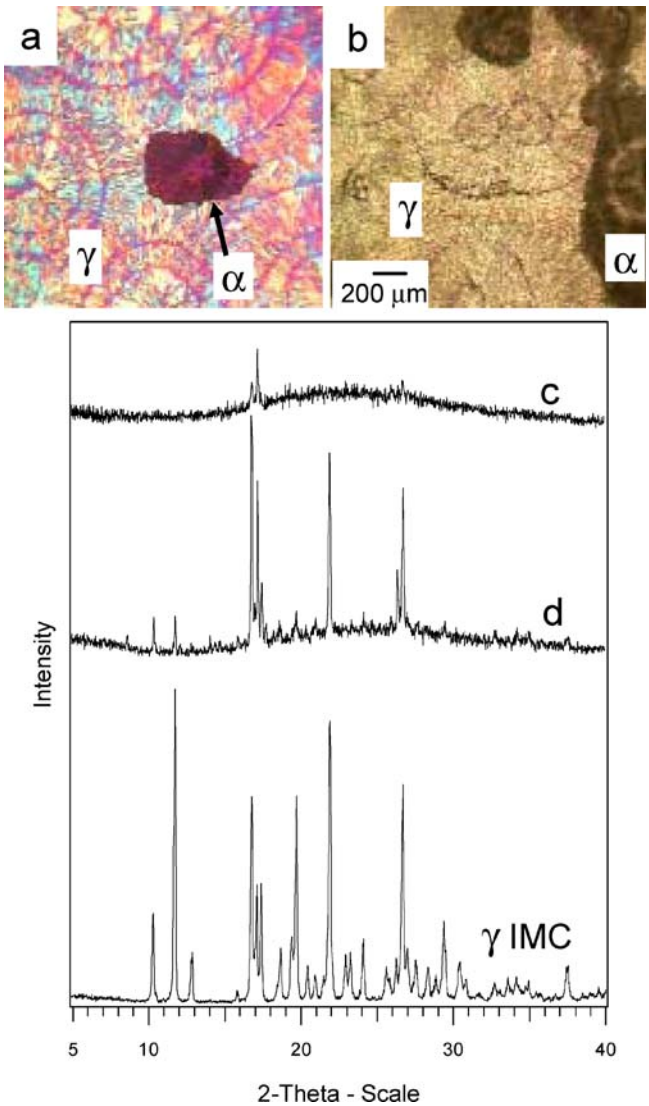

Fig. 2. Photomicrographs and XRPD patterns of crystals grown at the surface of amorphous IMC. **a** Complete surface coverage in 18 days. **b** Same as (**a**), but after 10 min at 140°C. **c** and **d** are XRPD patterns of (**a**) and (**b**).

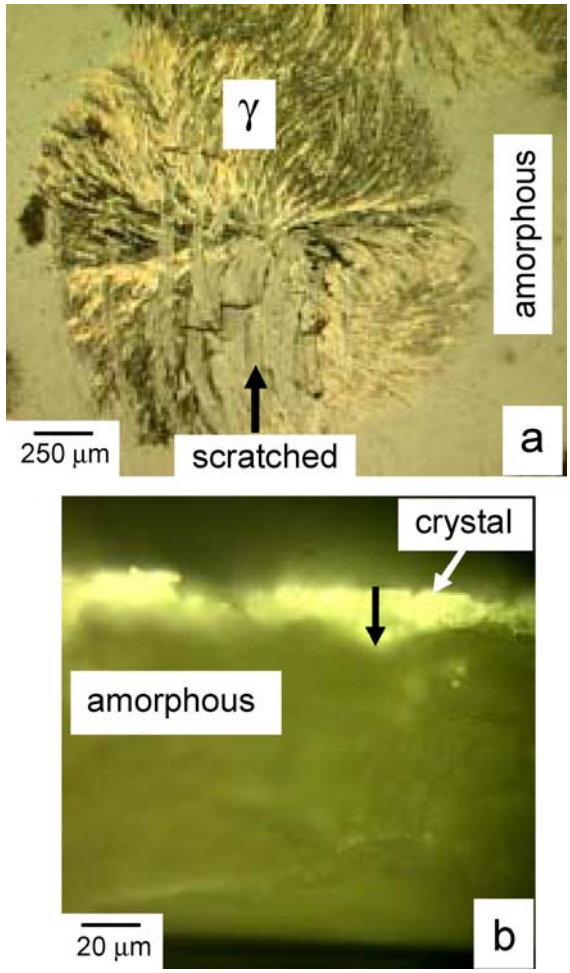

Fig. 3. **a** IMC crystals grown at the surface partially scratched off. **b** Cross-section of sample viewed between crossed polarizers. *Arrow* indicates direction of bulk growth.

thicker crystals (Fig. 2b). Thus, despite the apparent full coverage by crystals of the free surface, the sample in Fig. 2a was only partially crystallized and the crystals likely resided only at the free surface. The rings in the crystals in Fig. 2a and b resulted from temperature changes that the sample experienced when it was removed briefly from the 40°C chamber to the microscope at 22°C for observation.

To verify the surface crystallization of IMC, we scratched the crystals grown at the free surface of a thicker sample (130 μm). This exposed a non-birefringent amorphous material underneath (Fig. 3a). After a few days, new crystals again appeared in the scratched region. In another experiment, we cut the sample perpendicular to the free surface to expose its interior (Fig. 3b). Viewed between cross polarizers, the cross-section showed birefringent crystals residing only at the surface.

From the increase of the radii of IMC spherulites over time (Fig. 4a), we obtained the growth rates of γ and α IMC at the free surface (Fig. 4b). γ IMC grew slightly faster than α IMC. As shown in Fig. 4a, the growth rates decreased with time, which likely resulted from the physical aging of the amorphous solid and the resulting loss of molecular mobility. The growth rates in Fig. 4b corresponded to the data at the early stages of crystallization (lines of fitting in Fig. 4a). In

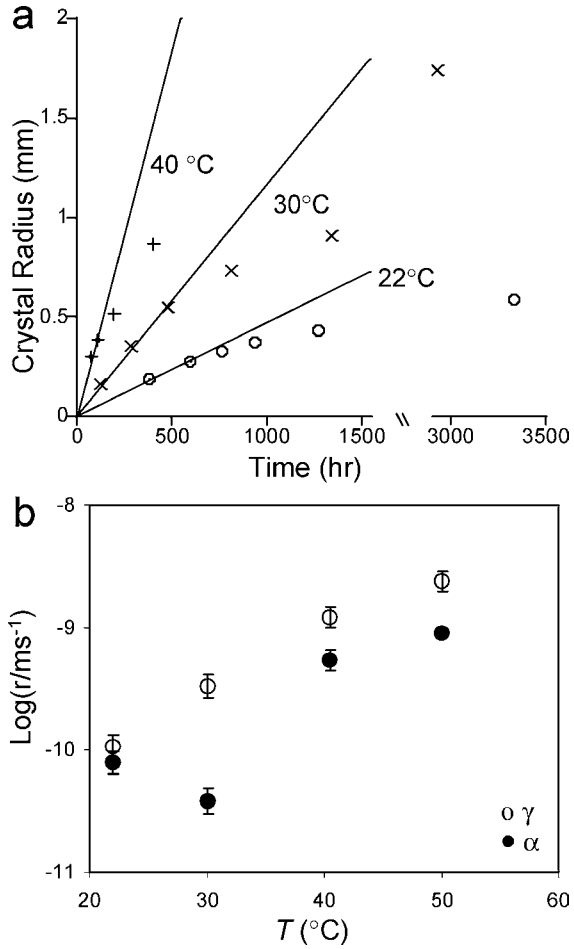

Fig. 4. **a** Representative data of crystal growth kinetics of γ IMC. *Lines* are fits to data at early stages of crystallization. **b** Crystal growth rates *vs.* temperature. *Error bar* is one standard deviation (n = 3).

comparison to these rates, the rates of crystal growth through the bulk (measured with samples between two cover glasses) were much slower. During the time the surface growth was measured, the bulk growth was not discernable. From much longer experiments, the bulk growth rate was estimated to be at least 100 times slower than the surface growth rate. The observed bulk growth rate was similar to the penetration rate of surface crystals into the bulk (arrow in Fig. 3b).

The results in Fig. 4b were obtained with IMC samples 15 μm thick. Because each sample was constrained at the bottom to the surface of a cover glass, we determined how the sample thickness affected the crystal growth rate. Figure 5 shows that this effect was modest for samples 15 μm thick. At this thickness, the free surface presumably did not sense the presence of the bottom cover glass. At thickness below 3 μm, however, the growth rate was significantly lower, presumably because the surface crystals had comparable thickness as the liquid sample.

Effect of Surface Crystallization on the Kinetics of Crystallization of Amorphous IMC Powder

The finding that the surface crystallization of IMC was faster than its bulk crystallization suggests an explanation for

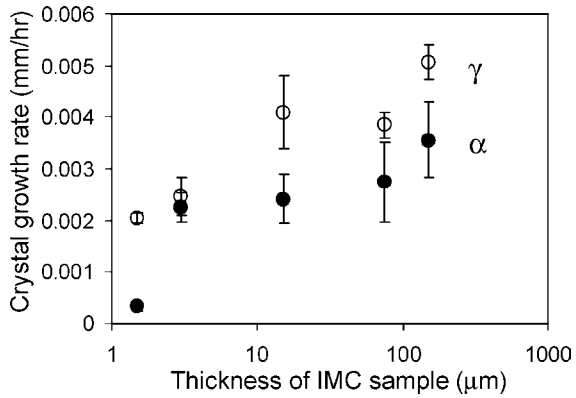

Fig. 5. Effects of sample thickness on surface growth rate at 40°C. The data correspond to thicknesses of 1.5, 3, 15, 75 and 150 μm. *Error bar* is one standard deviation (n = 3).

the apparent suspension of crystallization at 40°C after a rapid initial increase of crystallinity (8). To test this explanation, we stored amorphous IMC of three particle sizes (S, <75 μm; M, 75–250 μm; L, >250 μm) at 40°C for up to 20 days to determine their rates of crystallization. Figure 6

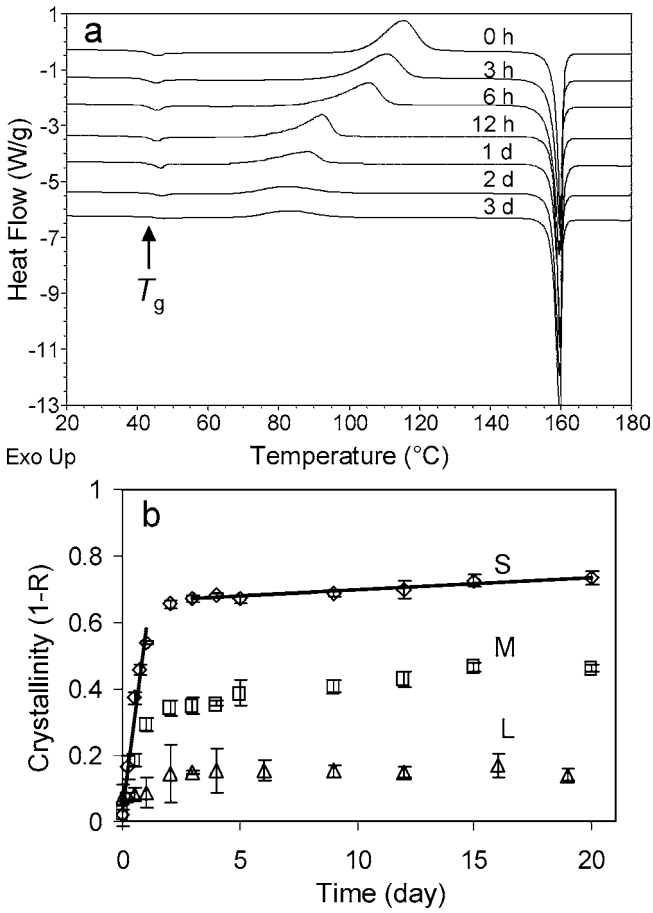

Fig. 6. **a** Representative DSC traces of amorphous IMC powder (Sample S) stored at 40°C for different times. Scan rate = 10°C/min. **b** Degree of crystallinity *vs.* time for ground IMC of small (*S*), medium (*M*), and large (*L*) particle sizes. *Lines* indicate crystallization rates at early and late stages. *Error bar* is one standard deviation (n = 3).

shows typical DSC data collected for this study. They featured a glass transition at 42°C, an exotherm of crystallization, and an endotherm of melting (159°C, of γ IMC). Figure 6b shows how the degree of crystallinity ($1-R$) increased at 40°C with storage time t (see Materials and Methods for details of calculation). All three samples showed rapid increase of crystallinity between 0 and 2 days, but the rate decreased subsequently. This finding agrees with that of Yoshioka *et al.* (8), who estimated the degree of crystallinity not by DSC, but by XRPD. The two lines drawn through the data points of Sample S illustrate the two rates of crystallization. The reduction in crystallization rate after 2 days was so great that the degree of crystallinity changed little in the remaining times and appeared "saturated" below 100%. With increasing particle size, the "saturation levels" decreased. These results agree with the conclusion that the abrupt suspension of crystallization resulted from the initially fast surface crystallization and the subsequently slow bulk crystallization.

Figure 7a shows a typical particle from Sample L after 3 days of storage at 40°C. Observation by PLM showed that this particle had fine crystals on its surface (Fig. 7b). We cut open this particle with a razor blade to expose its interior (Fig. 7c) and found that the interior was a smooth, non-birefringent amorphous mass containing no crystals. These observations again show that the IMC particles crystallized from the surface.

Figure 7d shows the XRPD patterns of Samples S, M, and L after sufficient times of storage at 40°C so that their degrees of crystallinity had reached "saturation levels." Sample L diffracted only weakly after 27 days, indicating incomplete crystallization, even though its surface was completely covered by crystals in 3 days. On going to Sample M and then to S, the XRPD peaks became stronger, indicating more complete crystallization. Nonetheless, these samples diffracted more weakly than a fully crystalline, commercial sample of γ IMC, indicating that they too were partially crystalline. Samples L, M, and S all crystallized as γ IMC.

Table I shows the glass transition temperatures T_g of the uncrystallized portions of Samples S, M, and L obtained when the samples were analyzed by DSC for degree of crystallinity (see Fig. 6a for representative data). The data for Samples S and M were obtained at 10°C/min and those for Sample L at 3–5°C /min (the slower rate was used to allow enough time for the sample to completely crystallize before melting). The T_gs of Samples S and M were similar and both increased slightly with storage time. This increase might have resulted from the relaxation of the glass during storage at 40°C. The lower T_gs of Sample L than those of Samples S and M resulted from the slower heating rate used for analyzing Sample L. The near constancy and slight increase of the T_gs in Table I indicate that the samples did not absorb a significant of amount of moisture during storage. It seems unlikely that moisture absorption during storage played a major role in the formation of surface crystals. Given the im-

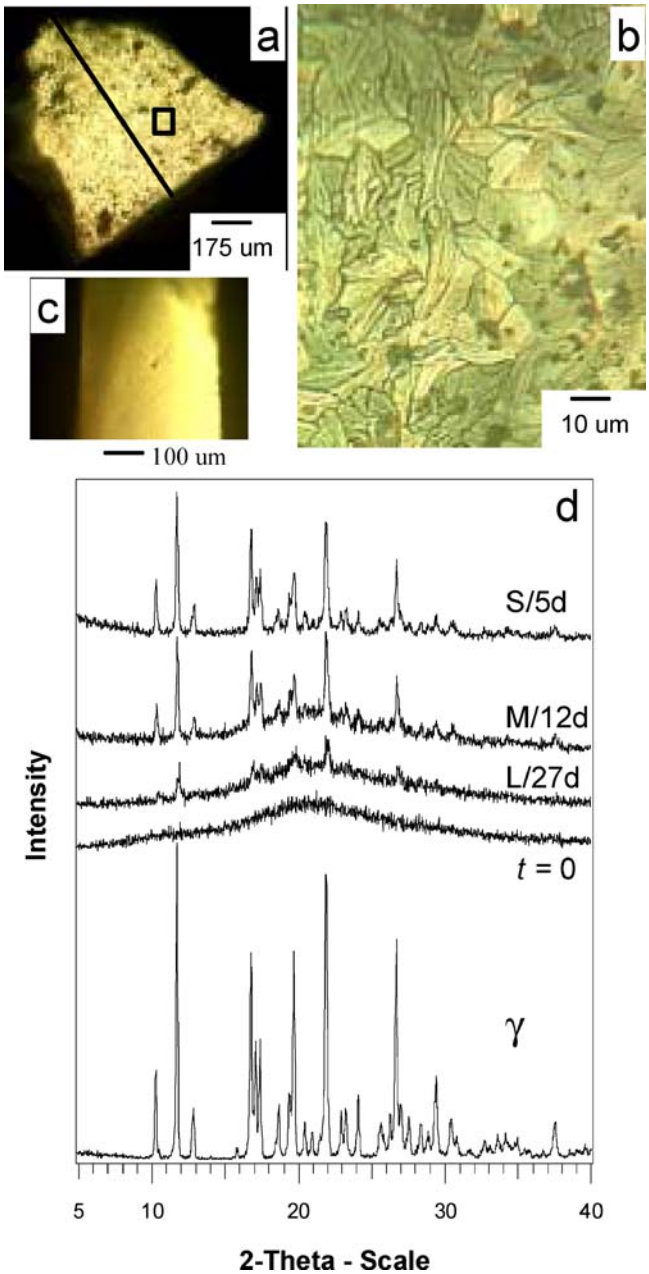

Fig. 7. **a** Typical particle of amorphous IMC after 3 days at 40°C. **b** *Enlarged view of rectangle* in (**a**) showing surface crystals. **c** Cross-section of particle in (**a**) (along the line in (**a**)) showing amorphous interior. (**d**) XRPD patterns of amorphous IMC powders after storage at 40°C compared with that of γ IMC. S/5d-Sample S/5 days.

Table I. Glass Transition Temperatures of Amorphous IMC of Different Particle Sizes Stored at 40°C

Storage time (day)	IMC		
	Small	Medium	Large
0	41.8 (0.8)	10.3 (1.6)	40.40 (0.2)
0.5	41.7 (0.2)	42.3 (0.2)	40.4 (0.2)
1	42.8 (0.4)	42.9 (0.2)	40.7 (0.4)
2	43.6 (0.3)	42.6 (0.5)	40.6 (0.5)
5	42.9 (1.4)	43.1 (0.6)	41.9 (0.2)
15	44.1 (0.3)	44.5 (0.2)	41.1 (0.1)

Standard deviation is in parenthesis (n = 3).

portance of moisture to drug stability, however, it is worthwhile to examine the effect of elevated humidity on surface crystallization.

The significantly faster surface crystallization of IMC than through the bulk may arise from the enhanced molecular mobility at the surface. This view seems consistent with other observations of surface crystallization and diffusion (1,2,15,16). In the case of IMC, faster surface crystallization than bulk crystallization leads to an abrupt suspension of crystallization after the material is partially crystallized (Fig. 6b) (8). The initial rapid crystallization (0–2 days) can be attributed to surface crystallization and the subsequent slow crystallization to bulk crystallization. The lower "saturation" crystallinity achieved by the sample of higher particle size can be attributed to its lower surface/volume ratio. For Sample S, we estimated the rates of crystallization in the early (surface) and late (bulk) phases (two lines in Fig. 6b) and found their difference to be about 150 times, which is similar to the estimated difference between the growth rates of surface and bulk crystals. The same phenomenon just discussed may explain the observation of suspended crystallization of pulverized amorphous phenobarbital (17).

It is noteworthy that the IMC polymorphs grow at different rates (Fig. 4b). On the free surface of amorphous IMC, the γ polymorph grows faster than the α polymorph. Such difference is not surprising given that polymorphs have different internal structures and growth morphologies. Such difference has been observed in other systems and been found to be a key factor controlling the pathways of crystallization (18,19). Today the ability to predict the relative growth rates of polymorphs is lacking, even with the knowledge of the crystal structures and thermodynamics of the polymorphs.

This study demonstrates the need to distinguish surface and bulk crystallization in modeling and controlling the stability of amorphous solids. Currently this distinction is rarely made. This distinction is especially important for understanding and predicting how particle size and surface characteristics affect the stability of amorphous solids. This distinction suggests new thinking about the optimal strategy to stabilize amorphous solids with faster surface crystallization than bulk crystallization.

CONCLUSIONS

We observed significantly faster crystal growth of IMC below T_g at the free surface than through the bulk. This phenomenon caused the unusual crystallization kinetics at 40°C wherein a rapid initial increase of crystallinity was followed by an abrupt slowdown of crystallization. This phenomenon also caused the IMC powder of higher particle size to reach lower "saturation level" of crystallinity. Surface crystallization of IMC yielded mainly the γ polymorph. Surface crystallization should be distinguished from bulk crystallization for modeling and controlling the crystallization of amorphous solids.

ACKNOWLEDGMENTS

We thank USDA (2005-01303) and University of Wisconsin for supporting this work and Profs. George Zografi and Mark Ediger for helpful discussions.

REFERENCES

1. P. W. McMillan. The crystallization of glasses. *J. Non-Cryst. Solids* **52**:(1–3), 67–76 (1982).
2. E. D. Zanotto. Experimental studies of surface nucleation and crystallization of glasses. *Ceram. Trans.: Nucleation and Crystallization in Liquids and Glasses* **30**:65–74 (1993).
3. D. Mahlin, J. Berggren, G. Alderborn, and S. Engstrom. Moisture-induced surface crystallization of spray-dried amorphous lactose particles studied by atomic force microscopy. *J. Pharm. Sci.* **93**:(1), 29–37 (2004).
4. T. Y. Shen, T. B. Windholz, A. Rosegay, B. E. Witzel, A. N. Wilson, J. D. Willett, W. J. Holtz, R. L. Ellis, A. R. Matzuk, S. Lucas, C. H. Stammer, F. W. Holly, L. H. Sarett, E. A. Risley, G. W. Nuss, and C. A. Winter. Nonsteroid antiinflammatory agents. *J. Am. Chem. Soc.* **85**:488–489 (1963).
5. C. A. Winter, E. A. Risley, and G. W. Nuss. Antiinflammatory and antipyretic activities of Indomethacin, 1-(*p*-chlorobenzoyl)-5-methoxy-2-methylindole-3-acetic acid. *J. Pharmacol. Exp. Ther.* **141**:(3), 369–376 (1963).
6. H. Imaizumi, N. Nambu, and T. Nagai. Stability and several physical properties of amorphous and crystalline form of indomethacin. *Chem. Pharm. Bull.* **28**:(9), 2565–2569 (1980).
7. E. Fukuoka, M. Makita, and S. Yamamura. Some physicochemical properties of glassy indomethacin. *Chem. Pharm. Bull.* **34**:(10), 4314–4321 (1986).
8. M. Yoshioka, B. C. Hancock, and G. Zografi. Crystallization of indomethacin from the amorphous state below and above its glass transition temperature. *J. Pharm. Sci.* **83**:(12), 1700–1705 (1994).
9. X. Chen, K. R. Morris, U. J. Griesser, S. R. Byrn, and J. G. Stowell. Reactivity differences of indomethacin solid forms with ammonia gas. *J. Am. Chem. Soc.* **124**:(50), 15012–15019 (2002).
10. S. Vyazovkin and I. Dranca. Physical stability and relaxation of amorphous indomethacin. *J. Phys. Chem. B* **109**:(39), 18637–18644 (2005).
11. M. Otsuka, T. Matsumoto, and N. Kaneniwa. Effect of environmental temperature on polymorphic solid-state transformation of indomethacin during grinding. *Chem. Pharm. Bull.* **34**:(4), 1784–1793 (1986).
12. M. Otsuka and N. Kaneniwa. A kinetic study of the crystallization process of noncrystalline indomethacin under isothermal conditions. *Chem. Pharm. Bull.* **36**:(10), 4026–4032 (1988).
13. K. J. Crowley and G. Zografi. Cryogenic grinding of indomethacin polymorphs and solvates: assessment of amorphous phase formation and amorphous phase physical stability. *J. Pharm. Sci.* **91**:(2), 492–507 (2002).
14. V. Andronis and G. Zografi. Crystal nucleation and growth of indomethacin polymorphs from the amorphous state. *J. Non-Cryst. Solids* **271**:(3), 236–248 (2000).
15. J. Schmelzer, R. Pascova, J. Moeller, and I. Gutzow. Surface-induced devitrification of glasses: the influence of elastic strains. *J. Non-Cryst. Solids* **162**:(1–2), 26–39 (1993).
16. R. Tromp. Surface diffusion: atoms go underground. *Nature Materials* **2**:(4), 212–213 (2003).
17. E. Fukuoka, M. Makita, and S. Yamamura. Glassy state of pharmaceuticals. III. Thermal properties and stability of glassy pharmaceuticals and their binary glass systems. *Chem. Pharm. Bull.* **37**:(4), 1047–1050 (1989).
18. S. Chen, H. Xi, and L. Yu. Cross nucleation between ROY polymorphs. *J. Am. Chem. Soc.* **127**:17439–17444 (2005).
19. J. Tao and L. Yu. Kinetics of cross-nucleation between polymorphs. *J. Phys. Chem. B* **110:**7098–7101 (2006).